9

High-field imaging of neurodegenerative diseases

M.J. Versluis
J. van der Grond
M.A. van Buchem
P. van Zijl
A.G. Webb

Neuroimaging Clinics of North America 2012; 22(2):159-71

ABSTRACT

High field magnetic resonance imaging is showing potential for imaging of neurodegenerative diseases. 7 T MRI is beginning to be used in a clinical research setting and the theoretical benefits, i.e. higher signal-to-noise, sensitivity to iron, improved MRA and increased spectral resolution in spectroscopy are being confirmed. Despite the limited number of studies to date, initial results in patients with multiple sclerosis, Alzheimer's disease and Huntington's disease show promising additional features in contrast that may assist in better diagnosis of these disorders.

INTRODUCTION

The increase in static magnetic field strength (B_0) for clinical MRI scanners has resulted in significant improvements in image quality. There is almost universal improvement in the diagnostic value of 3 T vs. 1.5 T clinical neurological MRI scans and 3 T scanners are routinely used for a broad range of applications. The need for increased sensitivity to early indicators of neurodegeneration with the goal of identifying potential biomarkers for diagnosis and the monitoring of treatment is one of the driving forces behind the interest in increasing further the magnetic field strength. The well-characterized signal-to-noise ratio (SNR) increase with field strength can be used for reduced acquisition times or higher spatial resolution. The increased sensitivity of image contrast (particularly in T_2*-weighted sequences) to tissue iron levels has great potential for detecting early diffuse depositions that may lead to neurotoxic effects. The longer T_1 value of both blood and tissue results in higher quality MR angiography (MRA) with improved background suppression. Furthermore, the increased chemical shift difference between the proton signals of different metabolites has an advantage for magnetic resonance spectroscopy (MRS) in quantifying more metabolites than previously possible (1, 2).

Initial imaging studies of multiple sclerosis (MS) patients at 7 T appear promising in detecting more lesions with higher structural detail (3–5), especially in gray matter. In addition to the improved spatial resolution and signal-to-noise, the increased contrast in MR angiography (6) and cortical layer contrast in T_2*-weighted imaging (7) have already demonstrated the potential of 7 T MRI. However, many intrinsic challenges remain to obtaining high quality MR data at field strengths of 7 T and above.

Challenges

The main challenges are related to creating a homogeneous magnetic field (B_0) and radiofrequency (RF) field B_1 over the entire brain. A higher magnetic field strength results in increased sensitivity to magnetic susceptibility induced field variations. On a microscopic scale this effect enhances the contrast within cortical layers (7, 8), basal ganglia (9), small venous structures (10–12) and results in greater white matter heterogeneity (13). However large-scale magnetic field variations induced by e.g. air-tissue interfaces (static) or respiration (dynamic) can lead to undesired signal loss and image deformations. Most modern high field MRI scanners are equipped with higher order shim gradients to improve the static field homogeneity. Careful optimization of sequence parameters and image correction algorithms has shown that it is

possible to acquire high quality images even from sequences such as echo planar imaging, which are particularly susceptible to static magnetic field inhomogeneities. Equally problematic, the amplitude of dynamically fluctuating magnetic fields caused by respiration or body movements also increases with field strength. It has been shown that corrections for these dynamic effects are possible both prospectively and retrospectively. Using dedicated hardware or sequences (14–16) image quality can be restored reasonably well.

Another fundamental challenge at 7 T is producing a highly homogeneous RF field, B_1, with high efficiency in order to minimize tissue heating. B_1 inhomogeneities are due primarily to the dielectric properties of tissue, which result in partial constructive and destructive interactions from RF wave behavior (17). Tissue conductivity produces conduction currents in tissue, which dampens the electromagnetic (EM) field as it penetrates through tissue, producing a phase shift in the travelling RF. This not only results in significant image inhomogeneity and areas of signal loss but may also give rise to local heating, expressed as the specific absorption rate (SAR) from interaction with the electric field. The dielectric properties of tissue produce displacement currents in tissue, as well as inductive losses caused by eddy currents, and also alter the RF wavelength in tissue. The effective wavelength of electromagnetic energy in tissue is ~13 cm at 7 T. The brain has dimensions on the same order as the wavelength. This limits the applicability of conventional volume coils, such as the birdcage (18) and transverse electromagnetic (TEM) resonator (19), which produce homogeneous transmit fields at 1.5 T and 3 T, but cannot produce the same homogeneous fields at 7 T (17). The inhomogeneous RF field in combination with increased tissue heating leads to important sequence considerations. SAR intensive protocols involving sequences such as fast spin echo and fluid attenuated inversion recovery (FLAIR) cannot simply be copied from lower field strengths. Solutions will be discussed in the section “Future prospects and challenges”.

Despite these challenges 7 T MRI is beginning to be used in a clinical setting and the theoretical benefits of 7 T, i.e. higher signal-to-noise, sensitivity to iron, improved MRA and spectroscopy are being confirmed. Although, so far only a limited number of patient studies have been performed at 7 T and many of the proposed techniques still need further validation. Initial imaging studies of multiple sclerosis (MS) patients at 7 T appear promising in detecting more lesions with higher structural detail (3–5), especially in gray matter. In addition to the improved spatial resolution and signal-to-noise, the increased contrast in MR angiography (6) and the detection of cortical

layer contrast in T_2*-weighted imaging (7) have already demonstrated the potential of 7 T MRI.

NEURODEGENERATIVE DISEASES

This section describes some of the clinical studies with 7 T MRI that have performed so far in patients suffering from neurodegenerative diseases.

CADASIL

Cerebral autosomal dominant arteriopathy with subcortical infarcts and leukoencephalopathy (CADASIL) is a hereditary form of small vessel disease that is caused by a mutation in the Notch3 gene. Pathologically, degeneration of the small smooth vessels is observed together with fibrous thickening of the small vessels. Clinical characteristics of the disease comprise cognitive loss, migrainous headaches, stroke-like episodes and dementia. In addition, cerebral blood flow is known to be reduced in CADASIL patients. However, the exact mechanism remains unclear and most findings regarding vessel wall pathology come from ex vivo studies. In vivo MRA can potentially provide valuable information on the hemodynamic changes in CADASIL patients. The most affected vessels are the leptomeningeal arteries supplying the white matter and the lenticulostriate perforating arteries supplying the deep gray nuclei. At lower field strengths MRA has been unable to visualize these arteries because of its small diameter. However, recent studies performed at 7 T show sufficient enhancements in resolution and contrast enabling visualization of the lenticulostriate arteries (6, 20, 21). The method that is most suited is time-of-flight (TOF) MRA, where the contrast is generated by the fresh inflow of blood with a gradient echo sequence that is relatively SAR friendly. The prolonged T_1 relaxation times at 7 T result in improved background saturation compared to lower field strengths, increasing the contrast between the vessel lumen and surrounding tissue. In addition the increase in SNR can be traded for a very high spatial resolution. In a recent study this was confirmed by visualization of significant lengths of the lenticulostriate arteries (22) in patients with CADASIL and control subjects. Figure 1 shows an example of a coronal maximum intensity projection of the lenticulostriate arteries in a healthy control subject and in a patient with CADASIL. The arrows point towards the lenticulostriate arteries. A small field of view (FOV) 3D TOF MRA technique was used with an isotropic resolution of 0.23 mm and 161 slices, resulting in a scan duration of 11 minutes. From these datasets, the number of visible arteries at different locations with respect to the middle and anterior cerebral artery, the cross-sectional area and length of the arteries were determined. No significant differences were found bet-

ween patients and controls in any of the measures. In addition no association was found between the luminal diameters and lacunar infarct load in the basal ganglia and basal ganglia hypointensities on separately acquired T_2-, T_2^*- or T_1-weighted scans (22). These results suggest that basal ganglia damage in CADASIL is likely not caused by vascular mechanisms. The lack of association between age and disease duration with these vascular measurements further supports the finding that generalized narrowing of luminal diameters of lenticulostriate arteries does not play a significant role in the pathophysiology of CADASIL.

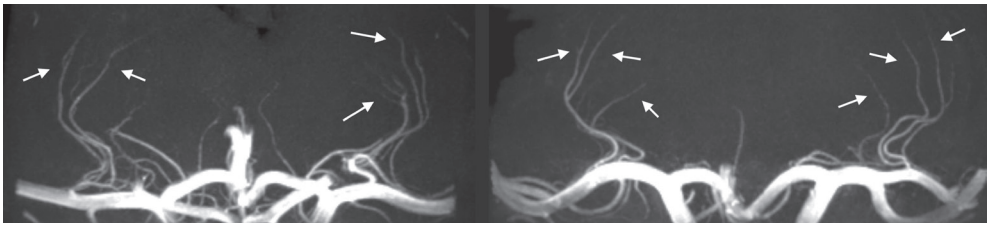

Figure 1: MRA of lenticulostriate arteries.
Coronal maximum intensity projections of a 32 year old healthy control (left) and 32 year old patient with CADASIL (right). The arrows point towards the lenticulostriate arteries. Excellent visualization of large portions of the lenticulostriate arteries was possible due to the high spatial resolution and contrast between the artery and surrounding tissue. No significant differences in length, diameter and number of lenticulostriate arteries was found, suggesting that basal ganglia damage in patients with CADASIL is not due to luminal narrowing of these vessels.

Another common MRI finding in patients with CADASIL are hypointensities on T_2*-weighted images (22, 23) caused by iron containing hemosiderin deposits in cerebral microbleeds (CMBs). Figure 2 show CMBs observed bilaterally in the thalamus of a 35 year old patient with CADASIL on a T_2*- and T_1-weighted image. Initial results have shown diffuse areas of T_2* hypointensity in the basal ganglia, most commonly caused by diffuse iron deposition in CADASIL (24). Such diffuse areas have been described in other neurodegenerative diseases such as Alzheimer's disease (AD) as well. Still, it is unsure whether iron deposition is exclusively a neurodegenerative process, or if it can also be caused by vascular mechanisms. High field T_2*-weighted MRI is extremely sensitive to changes in the local magnetic field, such as those generated by iron-rich regions. These changes in local magnetic field lead to decreased signal intensity on magnitude images and an increased frequency shift (relative to non-iron containing brain tissue) on phase images. Preliminary data of high resolution T_2*-weighted images using a 2D gradient echo sequence obtained with a resolution of 0.24x0.24x1 mm^3 (24), demonstrated increased iron deposition in the globus pallidus and the caudate nucleus.

These findings were based on both magnitude images and unwrapped phase images. Both approaches gave similar results but the phase shift measurements showed larger differences, emphasizing the sensitivity of phase to iron induced changes in the brain.

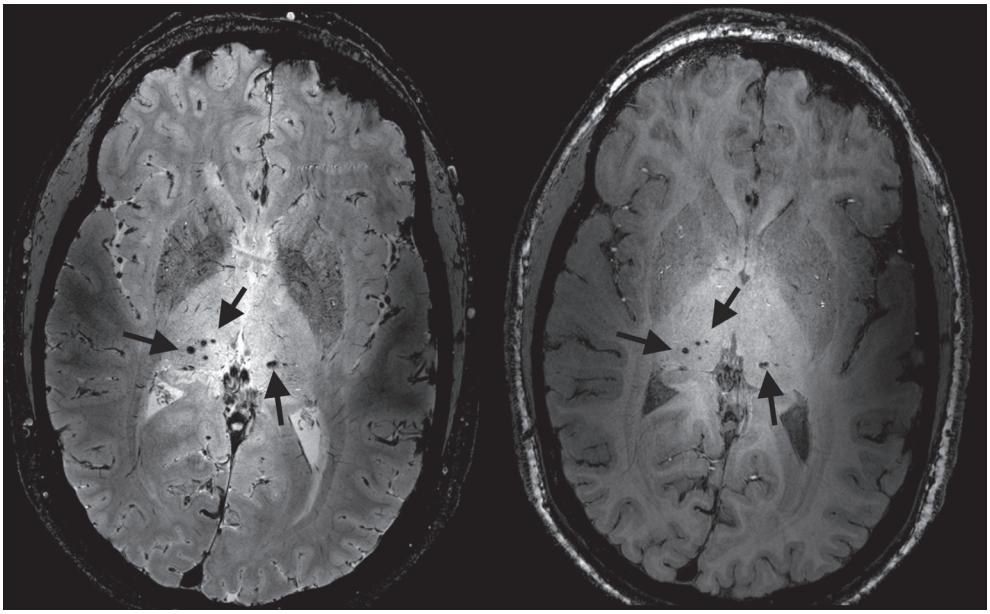

Figure 2: Microbleed detection in CADASIL.
Cerebral microbleeds (CMB) observed bilaterally in the thalamus of a 35 year old patient with CADASIL, visualized on a T_2*-weighted (left) and T_1-weighted (right) scan. The arrows point to the CMB. Accurate visualization of CMB is possible at high magnetic field strengths due to the induced susceptibility effect of haemosiderin deposits in the microbleeds. The sensitivity to detect CMB is highest on T_2*-weighted scans.

In summary, high field MRI can provide useful additional information in understanding CADASIL pathology given the high resolution TOF images, sensitivity to CMBs (25) and diffuse iron deposition.

Huntington's Disease

Huntington's disease (HD) is a neurodegenerative autosomal dominant disorder caused by a gene mutation on the short arm of chromosome 4. A repeat expansion of the cytosine-adenine-guanine gene leads to an abnormally increased synthesis of huntingtin, a protein causing neuronal damage and brain atrophy. Ultimately, the disease leads to functional disturbances of motor function, cognition and behavior. Brain atrophy measurements, particularly of the striatum, are considered the MRI hallmark of the disease, showing changes up to a decade before clinical manifestations of the disease oc-

cur. The exact disease mechanism underlying these volume changes remains unclear. Several proposed theories include impaired energy metabolism and the degeneration of neurons due to neuronal overstimulation (excitotoxicity). MRS offers additional insight into which processes may play a role in these volume changes, by measuring, for example, N-acetylaspartate (NAA), creatine and glutamate concentrations. If the neuronal integrity were to be compromised, NAA would be expected to be reduced. Changes in energy deposition may be reflected in total creatine signals. In contrast, an increase in glutamate levels would reflect overstimulation of neurons. Lower field MRS studies have shown conflicting results, especially for findings in glutamate concentrations (26). Higher field provides improved spectral resolution allowing more metabolites to be quantified (1, 2). This can be done with better spatial localization (smaller volumes) due to increased SNR. In a study by Van den Bogaard et al. (26) localized MRS was performed using a stimulated echo acquisition mode (STEAM) sequence in the caudate nucleus, putamen, thalamus, hypothalamus and frontal lobe in patients with manifest and premanifest HD. Using 7 T MRS six metabolites could be identified in all of these nuclei: choline, creatine, glutamine + glutamate, total NAA, myo-inositol and lactate, despite the significant brain atrophy, which lead to reduced SNR. Figure 3 shows MR spectra in the caudate nucleus and putamen of control subjects and manifest patients. Lower concentrations of creatine and NAA were found in the caudate nucleus and the putamen, and a reduction of glutamate in the putamen, of manifests HD patients. Secondly an association between disease severity and metabolic levels of NAA, creatine and glutamate was demonstrated. The results from this study indicate affected energy metabolism in HD patients reflected in lower creatine concentrations, and a decrease in neuronal integrity reflected in lower NAA concentrations. In contrast to other studies a lower concentration of glutamate was found in the putamen of manifest patients. This study showed that 7 T allows measurement of reliable glutamate concentrations, thereby obtaining additional insight in the disease process.

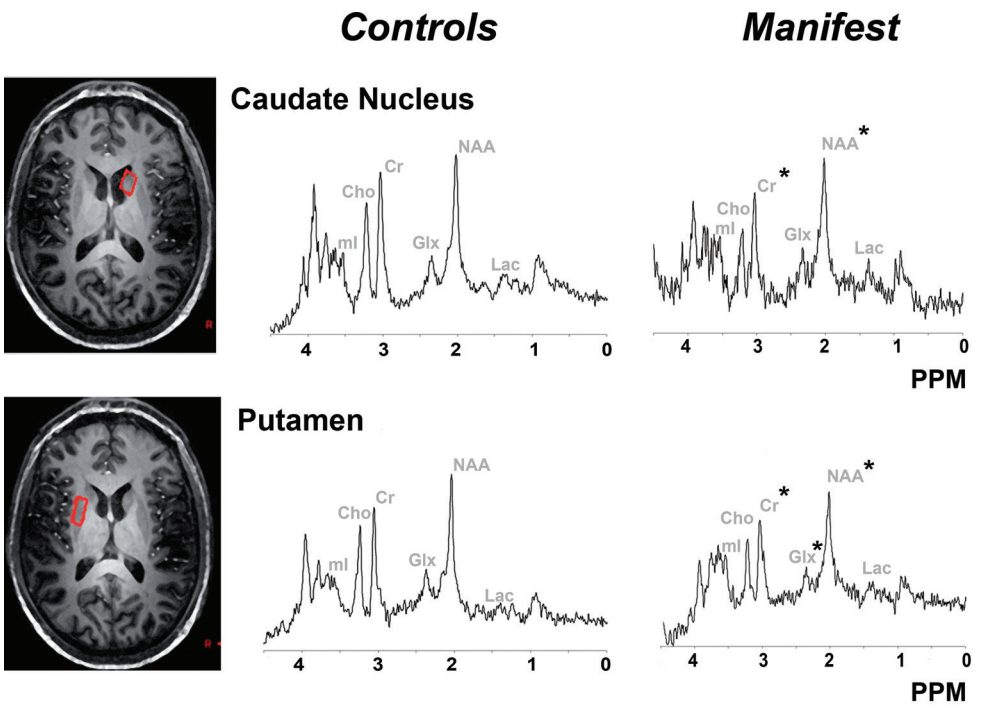

Figure 3: Representative MR spectra from the caudate nucleus and putamen in a control subject and manifest HD patient.
In total six metabolites could be identified in the hypothalamus, thalamus, caudate nucleus, putamen and the prefrontal region. In the caudate nucleus and putamen a significant decrease in NAA and creatine levels was found in manifest HD patients. Glutamate levels were found to decrease significantly in the putamen. Significance changes are depicted by asterisks (*), $p < 0.05$. ***Cho*** choline, ***Cr*** creatine, ***NAA*** N-acetylaspartate, ***mI*** myo-inositol, ***Glx*** glutamate + glutamine, ***Lac*** lactate, ***PPM*** parts per million.

In summary, the increased spectral and spatial resolution of 7 T MRS offer capabilities that are not possible at lower field strengths. It allows for the examination of metabolites in small anatomical structures in clinically acceptable scanning times, e.g. such as the caudate nucleus and putamen, which are important in many neurodegenerative diseases.

Multiple sclerosis

The field of MS research has been the most active since the introduction of 7 T MRI scanners. MS manifests itself through demyelinating lesions that can be detected by MRI. Conventional protocols use fluid attenuated inversion recovery (FLAIR) and dual inversion recovery (DIR) sequences to suppress signal from cerebrospinal fluid (CSF) or from both CSF and white matter, respectively, to highlight white matter (WM) lesions. In addition, gadolinium contrast agents can be administered to distinguish active lesions from older

lesions on T_1-weighted images. Histology has revealed that lesions not only occur in WM but also frequently affect gray matter (GM) and that MS lesions have a preference for a perivenular location. The high spatial resolution and sensitivity of high field facilitates the detection of GM lesions and the perivenous location of lesions, which is more difficult at lower field strengths.

To make effective use of the high contrast generated by venous blood and to circumvent the difficulties implementing B_1-sensitive and SAR-intensive sequences such as FLAIR and DIR, many studies have focused on T_2*-weighted sequences. Using this type of contrast it was found that between 50% and 87% of lesions contain a central vein (4, 5, 27–29). Compared to lower field strengths, a significantly lower number of lesions containing a central vein was found. At 1.5 T no central venous structure was observed in any of the detected lesions (4), whereas twice as many lesions with a central vein were detected at 7 T compared to 3 T (5). Figure 4 shows a large WM lesion visualized using T_2*-weighted MRI, comparing 7 T and 3 T (5). It is immediately apparent that the contrast within the lesion is enhanced at 7 T and that the perivenous location of the lesion can be appreciated.

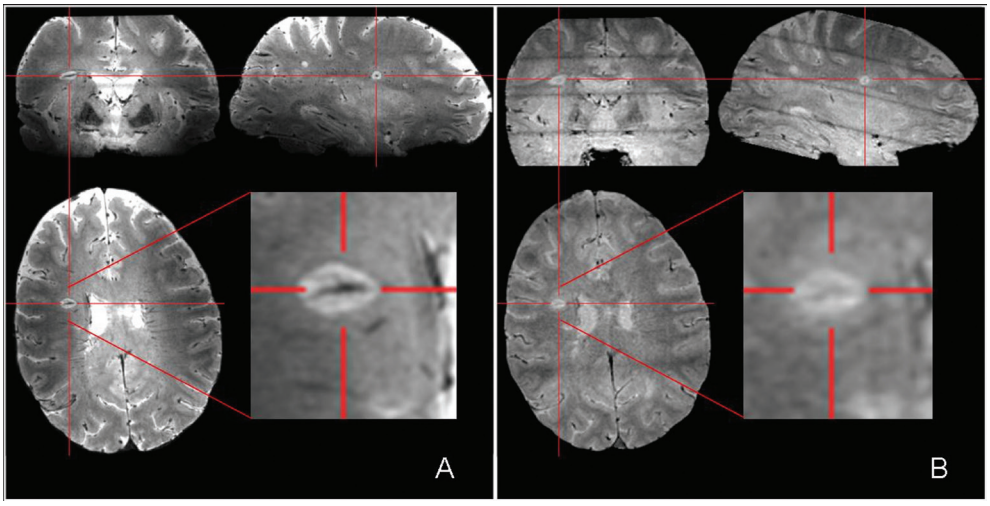

Figure 4: 7T T_2*-weighted MRI shows more detail of central veins in MS lesions than 3T. T_2* images of a patient with MS showing a large lesion with a perivenous orientation. On the 7T image (A) the vein can be seen in more detail than on the equivalent 3T image (B). Image courtesy of Dr. Emma Tallantyre.

The presence of a central vein in WM lesions may be an imaging characteristic that helps differentiating MS-related lesions from other WM lesions. This may be important for designing therapies targeted at MS lesions and monitoring disease progression, and also it may help providing insight into the mechanisms of lesion formation (27). It was found that the presence of

a central vessel is highly indicative of MS specific lesions. In a comparison between MS patients and subjects having WM lesions that were non-specific to MS, 80% of MS lesions had a perivenous location compared to only 19% in WM lesions not related to MS (29). The high sensitivity of 7 T in detecting perivascular signal changes is due to the susceptibility effect of venous blood. The effect of induced local magnetic field changes scales linearly with the applied magnetic field strength. Therefore the use of a sensitive method such as a T_2*-weighted sequence at high field greatly improves the contrast generated by venous blood.

Apart from WM lesions, GM lesions are also a frequent finding in MS. GM MS lesions, however, can be very difficult to detect at lower field strengths. The increased spatial resolution at 7 T increases the number of visible GM lesions. Figure 5 shows an example of an MS patient with a cortical GM lesion (30). The arrow in the zoomed in section points towards the cortical GM lesion. In one study no GM lesions could be detected in patients at 1.5T, while 44% of the lesions detected at 7T showed cortical involvement (4). This was confirmed by other studies at 7 T (30, 31). In line with other neurodegenerative diseases higher iron deposition is expected in patients with MS. The high sensitivity to iron of 7 T has lead to the investigation of MS lesions using phase images (3, 31, 32). However initial studies find that phase images have a lower sensitivity in detecting MS lesions (31) than the magnitude images. However between 8% and 21% of WM lesions show a characteristic ring around the lesion that is not readily visible on magnitude images (3, 31). This is thought to occur due to iron-rich macrophages and as such may provide information about the extent of inflammation around the MS lesion (4, 31).

T_2*-weighted sequences were identified as being the most sensitive in detecting lesions compared to other sequences (31) and lower field strength (4). Recently, progress has been made in reducing the SAR requirements of FLAIR and DIR sequences at 7 T while maintaining comparable or improved contrast and spatial resolution (33, 34). Preliminary results have shown the applicability in MS patients (35), although no systematic comparison of using high field FLAIR and DIR sequences has been published to date.

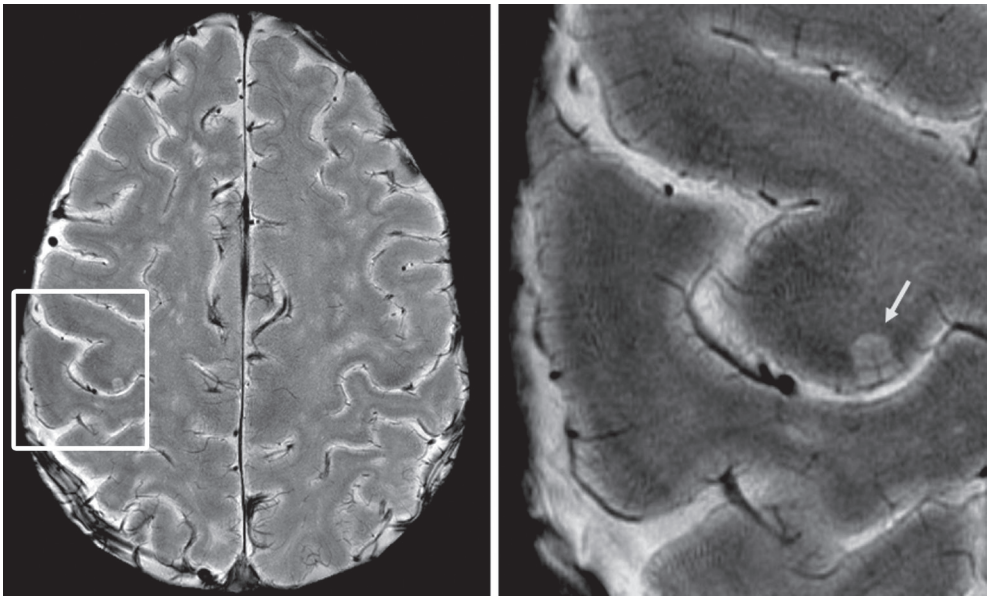

Figure 5: Axial T_2*-weighted image (195x260µm) of an MS patient with a cortical GM lesion at 7 T.
Right: Enlarged image of the region around the GM lesion demonstrating fine detail within the cortical lesion at this high magnetic field and fine spatial resolution. Image courtesy of Drs. Vigneron, Metcalf and Pelletier.

In summary, MS research at 7 T is promising. The difficulty in designing FLAIR and DIR sequences at 7 T has to date resulted in the use of T_2*-weighted sequences to detect MS lesions. The high contrast and spatial resolution of this sequence provides an additional type of sequence to investigate MS lesions, especially suited for high magnetic field strengths.

Other neurodegenerative diseases

There have been a number of other clinical studies in the field of neurodegenerative diseases at 7 T. Most studies use the same contrast mechanisms as mentioned in the previous sections. In amyotrophic lateral sclerosis (ALS) patients 7 T MRI was used to investigate the presence of CMBs. In animal models of this disease deposits of hemosiderin and CMBs were found, in contrast no CMBs were found in sporadic ALS patients (36). In patients with Alzheimer's disease (AD) a limited number of studies has been published. One of the hallmarks of AD is the presence amyloid beta plaques, a protein thought to be associated with iron. The small size of these plaques (typically smaller than 150 µm) (37) makes direct in vivo visualization difficult, although not impossible. Using localized coils and a limited FOV a resolution of the same order of magnitude as individual plaques has been obtained in

a reasonable scan time (38). Susceptibility weighted imaging (SWI) post processing was performed to enhance the sensitivity to susceptibility changes (39), such as induced by iron. The results of this study suggest that plaques can be visualized using this technique. Still, it remains unclear whether the observed signal voids represent individual plaques or not. In addition to the presence of plaques, early in the process of the disease brain atrophy occurs. One of the first brain regions affected by AD is the hippocampus; however not all subsections of the hippocampus are affected in a similar way. These different subregions can be distinguished using high resolution T_2*-weighted imaging sequences. One study has shown that in the very early stage of AD changes can be observed in the hippocampal subregion CA1 apical neuropil (40). From post mortem studies this region is known to be among the earliest affected in the brain. Interestingly at 7 T this was confirmed in vivo. Along the same line are findings in patients with hippocampal sclerosis (HS) where accurate visualization of subregions within the hippocampus is important for diagnosis. HS leads to atrophy of the intrahippocampal cortical fields CA1 to CA4 regions and to disruption of the internal hippocampal structure. In a study of focal epilepsy patients with HS, the intrahippocampal cortical fields could well be visualized on T_2- and T_2*-weighted sequences (41). Regional differences in hippocampal atrophy were shown between patients. In a different study similar findings were reported using T_1- and T_2-weighted imaging. In all patients hippocampal abnormalities were observed. Using 7 T MRI localized atrophy in the Ammon horn was observed in temporal lobe epilepsy patients (42).

A small number of patients with Parkinson's disease (PD) has been studied at 7 T. The symptoms of PD can sometimes be reduced by deep brain stimulation. This is a neurosurgical technique that relies on the accurate placement of electrodes. Using high-resolution susceptibility weighted imaging (SWI) high contrast can be generated between the iron rich basal ganglia. It has been shown that high quality images can be obtained that help guiding the placement of these electrodes (43, 44).

FUTURE PROSPECTS AND CHALLENGES

In general, the theoretical gain in SNR and sensitivity of high field MR to, for example, diffuse iron accumulation have been shown to be achievable in practice. Transmit RF field inhomogeneity is still a major concern, but by using dedicated sequences that are less sensitive to these inhomogeneities some of these effects can be circumvented (45, 46). By placing high dielectric materials close to the brain the transmit field becomes more homogeneous

(2, 47). The coverage towards the cerebellum in particular is improved and the effect of high signal centrally in the brain is reduced. The ultimate "solution", although currently only in the technical development phase, is the use of multiple transmit channels to improve the transmit homogeneity. Preliminary results already show the added value and one can anticipate that it will not take long before this technique is used in a clinical setting.

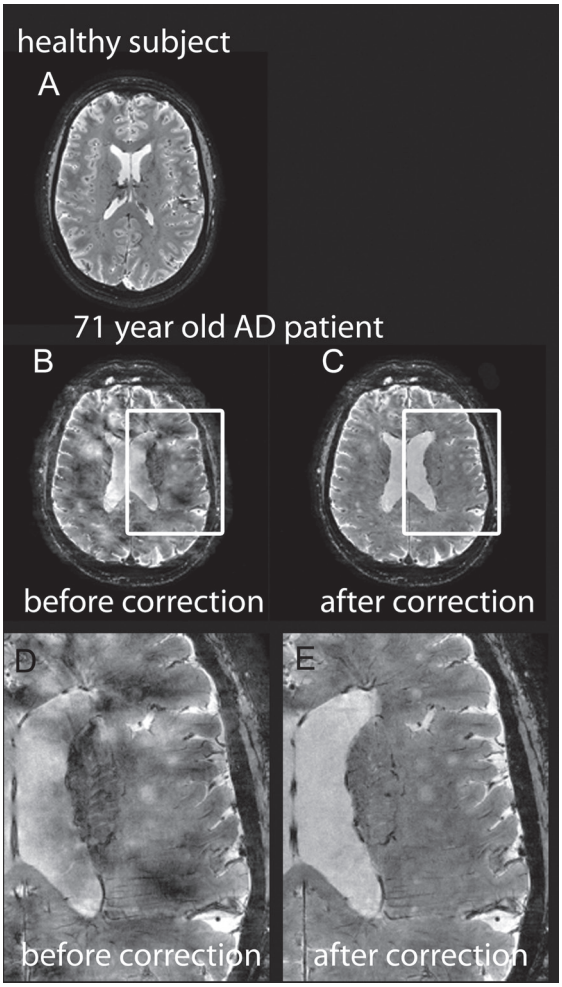

Figure 6: T_2*-weighted images before and after correction
A healthy subject (a), showing the high image quality and contrast that can be obtained. Application of the same sequence in patients with AD leads to frequent image degradation (b and d) caused by fluctuating magnetic fields during image acquisition. Using a navigator echo correction technique it is possible to measure and correct for these dynamic fluctuations and improve image quality significantly (c and e). Correction techniques like these improve image quality at high field.

Sequence adaptations have not been trivial, the increased RF deposition and inhomogeneous transmit field preclude the simple translation from lower field strength protocols to 7 T. However, all conventional image contrasts (T_1-, T_2-, T_2^*-weighted and FLAIR) are currently available with high image quality. To limit the need for additional lower field strength scans, it is important to have these image contrasts available.

Magnetic susceptibility induced field changes scale linearly with the applied field strength. This leads to an increased sensitivity to iron accumulation in the brain (8, 9) and WM heterogeneity (13) detected in T_2^*-weighted sequences. An adverse effect is that the sensitivity to unwanted field changes is also increased. Air tissue interfaces at the edge of the brain or near the sinuses generate a static inhomogeneous magnetic field. Shim gradients up to third order are used to compensate for these changes. However the effects of dynamic susceptibility changes are also enhanced, leading to ghosting and image blurring. It has been shown that breathing (14, 48) and body movements (49) can lead to substantial magnetic field changes in the brain. In a study in AD patients image artifacts were observed that were related to dynamic magnetic field changes (15). Figure 6 shows a transverse slice from a T_2*-weighted sequence in a healthy subject and an AD patient. The image quality is severely reduced in the AD patient. After navigator-based image correction for the effects of the magnetic field changes most image artifacts are suppressed. Still more advanced is to measure the field changes in real time using separate field probes that are positioned around the brain (16, 50), but this may not be clinically practical.

There has been rapid development of sequences and hardware since the introduction of 7 T MR systems. As a result most conventional sequences are available and high quality images are obtained in the brain. Based on the initial results so far, 7 T MRI is showing potential to be valuable in investigating neurodegenerative diseases. In patients with MS an increased number of lesions can be detected and more importantly, there is greater sensitivity to detect GM lesions. In addition to the increased sensitivity, also the pathophysiology of these lesions can be studied more extensively at high field. It was shown that most MS lesions have a clear vascular component. However, some lesions also showed up on phase images surrounded by a hypointense rim, possibly reflecting the area of inflammation or potentially a susceptibility effect. In patients with HD it was possible to quantify metabolite levels, including glutamate in very small regions of interest, providing valuable information about possible disease mechanisms. The sensitivity to iron and the high spatial resolution leads to a clearer depiction of the substantia nigra

and other deep gray matter nuclei in PD.

Even though limited clinical studies have been performed thus far, it is expected that the contribution of 7 T MRI especially in the field of neurodegenerative diseases will increase over time. Many of the initial problems related to magnetic and RF field inhomogeneities and the lack of optimized sequences have been solved or improved.

REFERENCES

1. Tkác I, Oz G, Adriany G, Uğurbil K, Gruetter R. In vivo 1H NMR spectroscopy of the human brain at high magnetic fields: metabolite quantification at 4T vs. 7T. Magn Reson Med 2009 ;62:868–879.
2. Mekle R, Mlynárik V, Gambarota G, Hergt M, Krueger G, Gruetter R. MR spectroscopy of the human brain with enhanced signal intensity at ultrashort echo times on a clinical platform at 3T and 7T. Magn Reson Med 2009 ;61:1279–1285.
3. Hammond KE, Metcalf M, Carvajal L, Okuda DT, Srinivasan R, Vigneron D, Nelson SJ, Pelletier D. Quantitative in vivo magnetic resonance imaging of multiple sclerosis at 7 Tesla with sensitivity to iron. Ann. Neurol 2008 ;64:707–713.
4. Kollia K, Maderwald S, Putzki N, Schlamann M, Theysohn JM, Kraff O, Ladd ME, Forsting M, Wanke I. First Clinical Study on Ultra-High-Field MR Imaging in Patients with Multiple Sclerosis: Comparison of 1.5T and 7T. AJNR Am J Neuroradiol 2009 ;30:699–702.
5. Tallantyre EC, Morgan PS, Dixon JE, Al-Radaideh A, Brookes MJ, Evangelou N, Morris PG. A comparison of 3T and 7T in the detection of small parenchymal veins within MS lesions. Invest Radiol 2009 ;44:491–494.
6. Kang C-K, Park C-W, Han J-Y, Kim S-H, Park C-A, Kim K-N, Hong S-M, Kim Y-B, Lee KH, Cho Z-H. Imaging and analysis of lenticulostriate arteries using 7.0-Tesla magnetic resonance angiography. Magnetic Resonance in Medicine 2009 ;61:136–144.
7. Duyn JH, van Gelderen P, Li T-Q, de Zwart JA, Koretsky AP, Fukunaga M. High-field MRI of brain cortical substructure based on signal phase. Proc Natl Acad Sci U S A 2007 ;104:11796–801.
8. Fukunaga M, Li T-Q, van Gelderen P, de Zwart JA, Shmueli K, Yao B, Lee J, Maric D, Aronova MA, Zhang G, Leapman RD, Schenck JF, Merkle H, Duyn JH. Layer-specific variation of iron content in cerebral cortex as a source of MRI contrast. Proceedings of the National Academy of Sciences 2010 ;107:3834 –3839.
9. Yao B, Li T-Q, Gelderen P van, Shmueli K, de Zwart JA, Duyn JH. Susceptibility contrast in high field MRI of human brain as a function of tissue iron content. NeuroImage 2009 ;44:1259–1266.
10. Conijn MMA, Geerlings MI, Luijten PR, Zwanenburg JJM, Visser F, Biessels GJ, Hendrikse J. Visualization of cerebral microbleeds with dual-echo T2*-weighted magnetic resonance imaging at 7.0 T. J. Magn. Reson. Imaging 2010 ;32:52–59.
11. Koopmans P, Manniesing R, Niessen W, Viergever M, Barth M. MR venography of the human brain using susceptibility weighted imaging at very high field strength. Magnetic Resonance Materials in Physics, Biology and Medicine 2008 ;21:149–158.
12. Theysohn JM, Kraff O, Maderwald S, Barth M, Ladd SC, Forsting M, Ladd ME, Gizewski ER. 7 tesla MRI of microbleeds and white matter lesions as seen in vascular dementia. J. Magn. Reson. Imaging 2011 ;33:782–791.
13. Li T-Q, van Gelderen P, Merkle H, Talagala L, Koretsky AP, Duyn J. Extensive heterogeneity in white matter intensity in high-resolution T2*-weighted MRI of the human brain at 7.0 T. NeuroImage 2006 ;32:1032–1040.
14. Van Gelderen P, de Zwart JA, Starewicz P, Hinks R, Duyn JH. Real-time shimming to compensate for respiration-induced B0 fluctuations. Magnetic Resonance in Medicine 2007 ;57:362–368.

15. Versluis MJ, Peeters JM, van Rooden S, van der Grond J, van Buchem MA, Webb AG, van Osch MJP. Origin and reduction of motion and f0 artifacts in high resolution T2*-weighted magnetic resonance imaging: Application in Alzheimer's disease patients. NeuroImage 2010 ;51:1082–1088.
16. Wilm BJ, Barmet C, Pavan M, Pruessmann KP. Higher order reconstruction for MRI in the presence of spatiotemporal field perturbations. Magnetic Resonance in Medicine 2011 ;65:1690–1701.
17. Webb AG, Collins CM. Parallel transmit and receive technology in high-field magnetic resonance neuroimaging. Int. J. Imaging Syst. Technol. 2010 ;20:2–13.
18. Hayes CE, Edelstein WA, Schenck JF, Mueller OM, Eash M. An efficient, highly homogeneous radiofrequency coil for whole-body NMR imaging at 1.5 T. J Magn Reson 1985 ;63:622–628.
19. Vaughan JT, Hetherington HP, Otu JO, Pan JW, Pohost GM. High frequency volume coils for clinical NMR imaging and spectroscopy. Magn Reson Med 1994 ;32:206–218.
20. Kang C-K, Park C-A, Kim K-N, Hong S-M, Park C-W, Kim Y-B, Cho Z-H. Non-invasive visualization of basilar artery perforators with 7T MR angiography. J Magn Reson Imaging 2010 ;32:544–550.
21. Zwanenburg JJM, Hendrikse J, Takahara T, Visser F, Luijten PR. MR angiography of the cerebral perforating arteries with magnetization prepared anatomical reference at 7T: Comparison with time-of-flight. Journal of Magnetic Resonance Imaging 2008 ;28:1519–1526.
22. Liem MK, van der Grond J, Versluis MJ, Haan J, Webb AG, Ferrari MD, van Buchem MA, Lesnik Oberstein SAJ. Lenticulostriate Arterial Lumina Are Normal in Cerebral Autosomal-Dominant Arteriopathy With Subcortical Infarcts and Leukoencephalopathy. Stroke 2010 ;41:2812 –2816.
23. Jouvent E, Poupon C, Gray F, Paquet C, Mangin J-F, Le Bihan D, Chabriat H. Intracortical Infarcts in Small Vessel Disease. Stroke 2011 ;42:e27 –e30.
24. Liem MKY, Oberstein SA., Versluis MJ, Haan J, Webb AG, Ferrari MD, van Buchem MA, van der Grond J. Diffuse iron deposition in the putamen and caudate nucleus in CADASIL: comparing phase and magnitude images at 7 Tesla. Proceedings of the International Society of Magnetic Resonance in Medicine. Montreal 2011 ;
25. Conijn MMA, Geerlings MI, Biessels G-J, Takahara T, Witkamp TD, Zwanenburg JJM, Luijten PR, Hendrikse J. Cerebral Microbleeds on MR Imaging: Comparison between 1.5 and 7T. AJNR Am J Neuroradiol 2011 ;32:1043–1049.
26. van den Bogaard SJA, Dumas EM, Teeuwisse WM, Kan HE, Webb A, Roos RAC, van der Grond J. Exploratory 7-Tesla magnetic resonance spectroscopy in Huntington's disease provides in vivo evidence for impaired energy metabolism [Internet]. J Neurol 2011 ;
27. Ge Y, Zohrabian VM, Grossman RI. Seven-Tesla Magnetic Resonance Imaging: New Vision of Microvascular Abnormalities in Multiple Sclerosis. Arch Neurol 2008 ;65:812–816.
28. Tallantyre EC, Brookes MJ, Dixon JE, Morgan PS, Evangelou N, Morris PG. Demonstrating the perivascular distribution of MS lesions in vivo with 7-Tesla MRI. Neurology 2008 ;70:2076–2078.
29. Tallantyre EC, Dixon JE, Donaldson I, Owens T, Morgan PS, Morris PG, Evangelou N. Ultra-high-field imaging distinguishes MS lesions from asymptomatic white matter lesions. Neurology 2011 ;76:534 –539.

30. Metcalf M, Xu D, Okuda DT, Carvajal L, Srinivasan R, Kelley DAC, Mukherjee P, Nelson SJ, Vigneron DB, Pelletier D. High-Resolution Phased-Array MRI of the Human Brain at 7 Tesla: Initial Experience in Multiple Sclerosis Patients. J Neuroimaging 2010 ;20:141–147.
31. Mainero C, Benner T, Radding A, van der Kouwe A, Jensen R, Rosen BR, Kinkel RP. In vivo imaging of cortical pathology in multiple sclerosis using ultra-high field MRI. Neurology 2009 ;73:941 –948.
32. Hammond KE, Lupo JM, Xu D, Metcalf M, Kelley DAC, Pelletier D, Chang SM, Mukherjee P, Vigneron DB, Nelson SJ. Development of a robust method for generating 7.0 T multichannel phase images of the brain with application to normal volunteers and patients with neurological diseases. NeuroImage 2008 ;39:1682–1692.
33. Zwanenburg J, Hendrikse J, Visser F, Takahara T, Luijten P. Fluid attenuated inversion recovery (FLAIR) MRI at 7.0 Tesla: comparison with 1.5 and 3.0 Tesla. European Radiology 2010 ;20:915–922.
34. Visser F, Zwanenburg JJM, Hoogduin JM, Luijten PR. High-resolution magnetization-prepared 3D-FLAIR imaging at 7.0 Tesla. Magn Reson Med 2010 ;64:194–202.
35. Visser F, Zwanenburg JJ, de Graaf WL, Castelijns JA, Luijten PR. 3D Magnetization Prepared Double Inversion Recovery (3D MP-DIR) at 7 Tesla. Proceedings of the International Society of Magnetic Resonance in Medicine. Montreal 2011 ;
36. Verstraete E, Biessels G-J, van Den Heuvel MP, Visser F, Luijten PR, van Den Berg LH. No evidence of microbleeds in ALS patients at 7 Tesla MRI. Amyotroph Lateral Scler 2010 ;11:555–557.
37. van Rooden S, Maat-Schieman MLC, Nabuurs RJA, van der Weerd L, van Duijn S, van Duinen SG, Natté R, van Buchem MA, van der Grond J. Cerebral Amyloidosis: Postmortem Detection with Human 7.0-T MR Imaging System. Radiology 2009 ;253:788–796.
38. Nakada T, Matsuzawa H, Igarashi H, Fujii Y, Kwee IL. In Vivo Visualization of Senile-Plaque-Like Pathology in Alzheimer's Disease Patients by MR Microscopy on a 7T System. Journal of Neuroimaging 2008 ;18:125–129.
39. Haacke EM, Xu Y, Cheng Y-CN, Reichenbach JR. Susceptibility weighted imaging (SWI). Magnetic Resonance in Medicine 2004 ;52:612–618.
40. Kerchner GA, Hess CP, Hammond-Rosenbluth KE, Xu D, Rabinovici GD, Kelley DAC, Vigneron DB, Nelson SJ, Miller BL. Hippocampal CA1 apical neuropil atrophy in mild Alzheimer disease visualized with 7-T MRI. Neurology 2010 ;75:1381 –1387.
41. Breyer T, Wanke I, Maderwald S, Woermann FG, Kraff O, Theysohn JM, Ebner A, Forsting M, Ladd ME, Schlamann M. Imaging of Patients with Hippocampal Sclerosis at 7 Tesla: Initial Results. Academic Radiology 2010 ;17:421–426.
42. Henry TR, Chupin M, Lehéricy S, Strupp JP, Sikora MA, Sha ZY, Ugurbil K, Van de Moortele P-F. Hippocampal Sclerosis in Temporal Lobe Epilepsy: Findings at 7 T [Internet]. Radiology 2011 ;
43. Abosch A, Yacoub E, Ugurbil K, Harel N. An Assessment of Current Brain Targets for Deep Brain Stimulation Surgery With Susceptibility-Weighted Imaging at 7 Tesla. Neurosurgery 2010 ;67:1745–1756.
44. Cho Z-H, Min H-K, Oh S-H, Han J-Y, Park C-W, Chi J-G, Kim Y-B, Paek SH, Lozano AM, Lee KH. Direct visualization of deep brain stimulation targets in Parkinson disease with the use of 7-tesla magnetic resonance imaging. Journal of Neurosurgery 2010 ;113:639–647.

45. Moore J, Jankiewicz M, Zeng H, Anderson AW, Gore JC. Composite RF pulses for -insensitive volume excitation at 7 Tesla. Journal of Magnetic Resonance 2010 ;205:50–62.
46. Henning A, Fuchs A, Murdoch JB, Boesiger P. Slice-selective FID acquisition, localized by outer volume suppression (FIDLOVS) for (1)H-MRSI of the human brain at 7 T with minimal signal loss. NMR Biomed 2009 ;22:683–696.
47. Haines K, Smith NB, Webb AG. New high dielectric constant materials for tailoring the distribution at high magnetic fields. Journal of Magnetic Resonance 2010 ;203:323–327.
48. Van de Moortele PF, Pfeuffer J, Glover GH, Ugurbil K, Hu X. Respiration-induced B0 fluctuations and their spatial distribution in the human brain at 7 Tesla. Magnetic Resonance in Medicine 2002 ;47:888–895.
49. Barry RL, Williams JM, Klassen LM, Gallivan JP, Culham JC, Menon RS. Evaluation of preprocessing steps to compensate for magnetic field distortions due to body movements in BOLD fMRI. Magnetic Resonance Imaging 2010 ;28:235–244.
50. Barmet C, Zanche ND, Pruessmann KP. Spatiotemporal magnetic field monitoring for MR. Magnetic Resonance in Medicine 2008 ;60:187–197.